15TH IEA HEAT PUMP CONFERENCE
MAY 26–29, 2026 | HOFBURG
VIENNA 2026
DECARBONISATION THROUGH INNOVATION

Part-load strategies for a steam-generating ejector heat-pump using numerical simulations

Julian Unterluggauer [a,*], Manuel Schieder[a], Michal Rezucha[a], Verena Sulzgruber[a], Michael Lauermann[a]

[a]AIT Austrian Institude of Technology GmbH, Giefinggasse 4, 1210 Vienna, Austria

Abstract

Steam-generating heat pumps are a promising solution for decarbonizing industrial processes, but their efficiency decreases significantly with high temperature lift. The resulting high-pressure differences between the condenser and evaporator lead to significant expansion losses in the Carnot cycle. This study investigates the use of an ejector as an alternative to the conventional throttle valve to improve the efficiency of steam-generating heat pumps under variable load conditions. A CFD-based homogeneous equilibrium model is used to simulate the ejector's performance and develop a flexible ejector concept for fluctuating steam demand. The results show that incorporating a needle into the motive nozzle reduces heat capacity while maintaining performance. Swirl control is an ineffective solution as subcooling increases (> 10K), which, however, is necessary in this case to enhance the performance of the heat-pump. Simulations of the needle ejector demonstrate stable operation down to 50% of full heat capacity. To further reduce capacity, a motive nozzle bypass is proposed.
The study indicates a COP improvement potential ranging from 30% to 10% across 100%-30% load conditions. The concept is demonstrated in a feed mill use case, where reduced steam production and a storage concept are required to handle recipe changes. The heat pump's condenser acts as a short-term steam buffer, requiring a 40% increase in shell diameter. Incorporating the ejector is essential to meet economic targets (ROI < 5 years).

Keywords: Steam heat-pump, CFD, Ejector

1. Introduction

Decarbonizing industrial processes is a critical step toward achieving a sustainable future. Since fossil-fuel-generated steam is the most widely used heat transfer medium in industry [1], the integration of steam-generating heat pumps (SGHP) presents a promising solution for supplying process heat in a sustainable and energy-efficient manner. Instead of expanding high-pressure steam produced by fossil-fired boilers, SGHPs generate steam by upgrading waste heat, thereby achieving significantly lower exergy losses. Therefore, a closed bottom cycle high temperature heat pump is used, which boosts a typical source temperature of 50°C to 120°C saturated steam using a condenser/evaporator. To produce higher steam temperatures and pressure, advantageous mechanical vapor recompression (MVR) units are used.
The MVR is well-developed and ensures high efficiency, but when considering the Carnot cycle of the heat pump, there is still room for improvement. The isentropic efficiency of the compressor is often the first factor considered and has therefore been extensively researched in the past. However, the most influential component in terms of efficiency is the expansion valve, which can be seen as a source of exergy loss. To recover some of these losses, the introduction of an ejector into the refrigerant cycle presents a promising solution. It bears

* Corresponding author. Tel.: +43 50550-6602; fax: +43 50550-6679
E-mail address: julian.unterluggauer@ait.ac.at

15th IEA Heat Pump Conference 2026 - ICO3.5 - https://doi.org/10.23697/1sk0-pv39

the potential to reduce the compressor work by increasing the suction pressure to a higher level, which decreases the compressor pressure ratio and directly leads to an improvement of the COP. The technology itself is far from new, as Kornhauser [2] has analyzed the thermodynamic performance of the ejector expansion refrigeration cycle using R12 as a working fluid in 1990.

Since then, experiments and Computational fluid dynamics (CFD) simulations were used to further develop the component and its integration especially for the use in CO_2 refrigeration cycles. Elbel and Lawrence concluded in their studies [3] [4] that a COP improvement in the range of 10 to 30% can be achieved. However, while it is a promising solution for improvements at the design conditions of the cycle, the performance severely suffers under off-design conditions [5] such as reduced capacity or temperature [6]. This functionality is crucial for integrating ejector technology into steam-generating heat pumps, as steam demand often varies.

In this work, a combined 1D/2D-CFD approach is used to design an ejector for a R600 (n-butane) SGHP, evaluating options that can provide performance improvements, even under part-load conditions such as reduced capacity.

2. Heat-pump

2.1. Refrigerant cycle

The working principle of an ejector is, that a high-pressure liquid enters the motive inlet where it is further accelerated to super-sonic speed in a converging-diverging nozzle. After the nozzle the accelerated and partially evaporated refrigerant enters the mixing section, creating a pressure environment which has a lower pressure than the gaseous refrigerant on the suction inlet and therefore the refrigerant on the suction side gets entrained. In the mixing section momentum and energy is transferred and the flow reaches a sub-sonic state before entering the diffusor, in which the kinetic energy is converted to reach an outlet pressure intermediate between the motive and suction pressure. This pressure increase directly influences the coefficient of performance (COP) by reducing the necessary pressure lift for the compressor, and as a result, the electrical energy consumption.

There are several ways on how to adapt the SGHP cycle for the use of an ejector [4][5]. In this study the configuration as presented in Figure 1 was chosen.

To prevent liquid carryover into the compressor (1), the working fluid enters in a slightly superheated state. The high-pressure fluid (2) subsequently condenses (2–3), releasing heat for steam generation on the sink side, before passing through a subcooler (3–4). This subcooling step improves the coefficient of performance (COP) by preheating the feedwater prior to the fluid entering the internal heat exchanger (IHEX) (4). In the IHEX, the fluid is subcooled further before entering the ejector (5), while simultaneously superheating the fluid before the compressor (10-1) to ensure safe operation. Inside the ejector, low-pressure vapor from the source cycle (9) is entrained and compressed to a higher pressure level (6). The resulting two-phase mixture flows into a flash tank, where the vapor phase is separated and directed to the compressor (10), and the liquid phase is

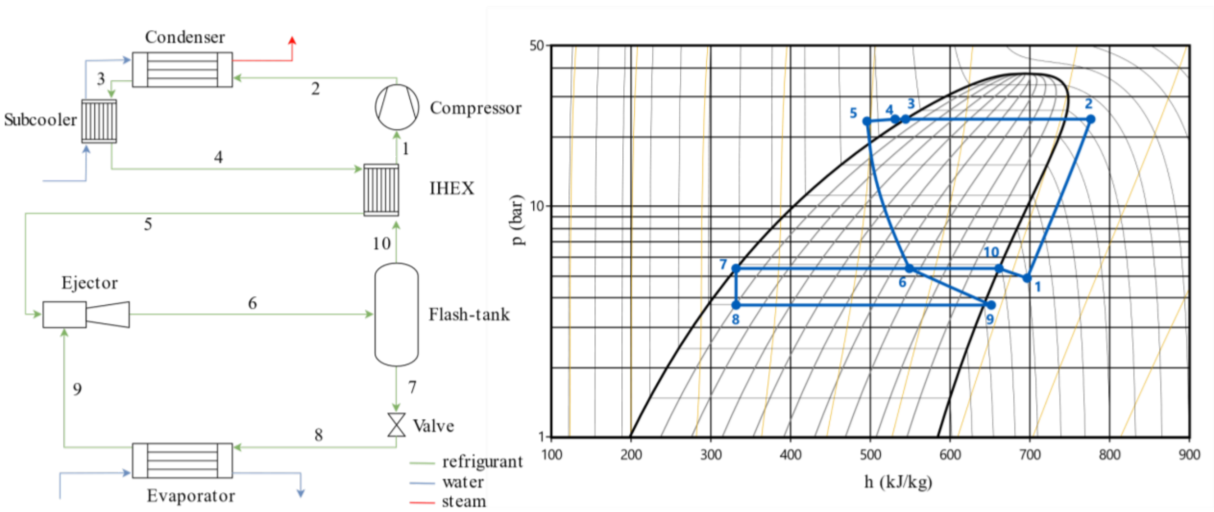

Figure 1.Heat-pump cycle and corresponding log(p)-h diagram

The ejector can be characterized by its entrainment ratio, which is a measure for the ejector's mass entrainment:

$$X = \frac{\dot{m}_{SN}}{\dot{m}_{MN}}, \tag{1}$$

with $\dot{m}_{SN}$ being the entrained mass flow at the suction inlet and $\dot{m}_{MN}$ the mass flow entering the motive nozzle.
Moreover, another important parameter is the ejector suction pressure ratio, which is a measure for the pressure lift:

$$\Pi_s = \frac{p_{out}}{p_{SN}}, \tag{2}$$

with p_{out} denoting the pressure at the ejector outlet and p_{SN} the pressure at the suction inlet.
Regarding the efficiency of the ejector, there are several ways in which it can be defined [6]. In this paper the ejector efficiency definition from Elbel and Hrnjak [7] is used:

$$\eta_{ej} = \frac{h(p_{out}, s_{SN}) - h_{SN}}{h_{MN} - h(p_{out}, s_{MN})} . X \tag{3}$$

The enthalpy is denoted by h, the entropy by s and the entrainment ratio by X.
This definition of the ejector efficiency has the advantage that all parameters can be directly obtained from measurements. Typically, this ejector efficiency ranges from 10 - 30% for transcritical CO_2 heat-pump cycles as stated by Elbel and Lawrence [5].
However, for the design process of the ejector using CFD and 1D heat cycle simulations, nozzle- and diffusor efficiencies were chosen:

$$\eta_{MN} = \frac{h_{MN,in} - h_{MN,out}}{h_{MN,in} - h^{s}_{MN,out}} \tag{4}$$

$$\eta_{DIF} = \frac{h^{s}_{DIF,out} - h_{DIF,in}}{h_{DIF,out} - h_{DIF,in}} \tag{5}$$

2.2. Part-load solutions

For the SGHP, part-load operation is defined as a reduction in the steam mass flow. This can also be achieved by reducing the refrigerant mass flow, which depends on the motive inlet conditions and the geometry of the ejector, especially the throat area. As stated by Zhu et al. [8], there are several methods to achieve mass flow control. One option is expansion valve control, which can be applied in both single and multi-ejector systems. In a multi-ejector setup, solenoid valves regulate the inflow and outflow of parallel ejectors, allowing for discrete part-load stages. However, in single ejector configurations, the range of controllability is limited by the degree of subcooling at the design point, since the working fluid is required to remain in the liquid phase upon entering the ejector. The multi-ejector approach is useful when predefined part-load steps are sufficient. However, to enable a wider and more flexible operating range, a variable nozzle geometry is suggested.
This adjustment can be realized by varying the diameter of the motive nozzle throat with a movable needle, as demonstrated by Elbel et al. [7] for CO_2. While effective, this approach is mechanically complex and introduces additional frictional losses, which can reduce system efficiency. These drawbacks are particularly pronounced in CO_2 ejectors used for refrigeration cycles, where the devices are relatively small. In such systems, even minor variations in needle position can cause substantial changes in mass flow, and the fine geometry of the needle may lead to oscillations. In contrast, the ejector proposed in this study is significantly larger, thereby eliminating these issues.

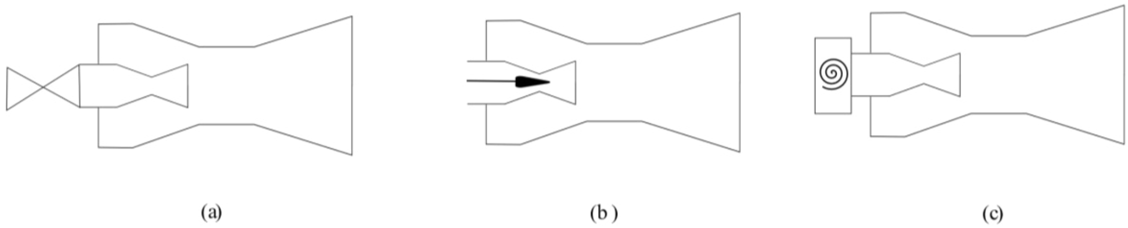

Figure 2. Ejector control by (a) expansion valve (b) needle (c) swirl

Furthermore, to address these limitations in CO_2, Zhu et al. [8] proposed an alternative method based on varying the vortex strength at the motive inlet. This approach enabled a maximum mass flow control of up to 42% in CO_2 ejectors. However, Bodys et al. [9] noted that this method is only effective at high rotational speeds at the motive inlet, which may limit its applicability in some systems.

3. Numerical Model

3.1. Geometry and Mesh for CFD

The geometry is designed by using a combined 1D & 2D simulation approach published by Unterluggauer et al. [10].

Motive nozzle (A)	$D_{MN,1}$ (mm)	104.4
	$D_{MN,2}$ (mm)	16.2
	$D_{MN,3}$ (mm)	36.4
	$D_{MN,4}$ (mm)	116.2
	$\gamma_{MN,1}$ (°)	12
	$\gamma_{MN,2}$ (°)	5
	$\gamma_{MN,3}$ (°)	37
Mixing chamber (C)	L_{MCH} (mm)	50
Suction nozzle (B) and Diffusor (D)	D_{SN} (mm)	181
	γ_{SN} (°)	18.5
	D_{MIX} (mm)	70
	L_{MIX} (mm)	501
	D_{DIF} (mm)	161
	γ_{DIF} (°)	2.5

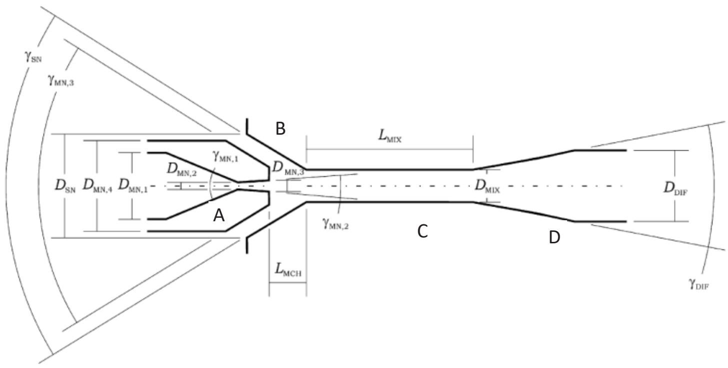

Figure 3. Ejector design

The domain is meshed using Ansys ICEM 2024R2 to generate a fully hexahedral grid with 970,000 cells. The maximum skewness is kept below 0.5, and refinements are applied at the walls to maintain a reasonable wall distance, ensuring that the y+ value is kept low (area-weighted average < 1). For needle control, a 10 mm needle with a 10° angle is inserted into the motive nozzle, providing a total adjustment range from 0 mm to 38.9 mm. A grid independency study on a very similar geometry using the same numerical setup and model has been published in the diploma thesis of Manuel Schieder [11].

3.2. Numerical Model and Boundary conditions for CFD

The boundary conditions are chosen according to the need of a SGHP around 1 MW of steam and are summarized in Table 1. ANSYS Fluent is employed as the solver for steady-state simulations The case is set up as axisymmetric for the needle control configuration and as three-dimensional for the swirl (vortex) control. For modeling phase transition, the Homogeneous Equilibrium Model (HEM) developed by Smolka [12] is used. It requires the energy equation to be solved in the enthalpy-based form. As by default Fluent uses the temperature-based form, this has to be done with a User Defined Scalar (UDS), solving an additional transport equation for the enthalpy. Material properties are updated through a User Defined Function (UDF), which performs bicubic spline interpolation to extract fluid properties from the material database TLK-ThermoLib based on Refprop data [13]. To model turbulence the k-ω-SST, taking compressibility effects into account, is used. All equations are discretized using first-order upwind schemes, except for pressure, where a second-order pressure interpolation scheme is applied.

Table 1 Design point of the R600 ejector

Boundary Condition	Value
Motive inlet total pressure (bar)	23.59
Motive inlet subcooling ΔT (K)	12.8
Secondary inlet total pressure (bar)	3.77
Secondary inlet superheating ΔT (K)	5
Outlet static pressure (bar)	5.34

One of the great advantages of using the HEM as a two-phase model is the low computational costs as the fluid is treated as single phase. The liquid and the vapor phase are assumed to be in a thermal and mechanical equilibrium, meaning that pressure, temperature, velocity, turbulence kinetic energy and turbulence dissipation rate are the same in both phases [12].
As previously mentioned, the thermodynamic properties are functions of specific enthalpy and pressure. This dependence necessitates the implementation of a UDS transport equation in ANSYS Fluent. The equation, formulated in terms of Favre-averaged quantities (denoted by a tilde) and Reynolds-averaged quantities (denoted by a macron), takes the following general form [12]:

$$\boldsymbol{\nabla} \cdot \left(\rho \tilde{\boldsymbol{u}} \tilde{\phi}\right) = \boldsymbol{\nabla} \cdot \left(\Gamma \boldsymbol{\nabla} \tilde{\phi}\right) + \dot{S}_{\phi}, \tag{6}$$

with $\dot{S}_{\phi}$ being an additional source term of an arbitrary scalar ϕ and Γ the diffusion of the same quantity ϕ. Based on this, the energy equation for the implementation in Ansys Fluent has the following form, according to [14]:

$$\boldsymbol{\nabla} \cdot \left(\rho \tilde{\boldsymbol{u}} \tilde{h}\right) = \boldsymbol{\nabla} \cdot \left(\Gamma_h \boldsymbol{\nabla} \tilde{h}\right) + \dot{S}_{h1} + \dot{S}_{h2} + \dot{S}_{h3}, \tag{7}$$

with Γ_h being the diffusivity of h:

$$\Gamma_h = \frac{\lambda}{c_p} + \frac{\mu_t}{\sigma_t}. \tag{8}$$

where λ denotes the thermal conductivity, c_p the specific heat capacity at constant pressure, μ_t the turbulent viscosity and σ_t the turbulent Prandtl number.
The source terms represent the mechanical energy $\dot{S}_{h1}$, the irreversible dissipation of kinetic energy variations $\dot{S}_{h2}$ and the dissipation of turbulent kinetic energy $\dot{S}_{h3}$.

3.3. Numerical Model for Heat-pump simulations

The heat pump cycle, including essential components such as the compressors, heat exchangers and flash tank, is modelled using the acausal, object-oriented, equation-based open-source modelling language Modelica. It allows for the convenient and efficient modelling of the dynamic behavior of physical systems, using a combination of differential, algebraic, and discrete equations. The simulations of the refrigeration circuit were performed using the TIL Library 3.10.0 (developed by TLK Thermo GmbH, Braunschweig, Germany) within the Dymola 2023x simulation environment. All components in the refrigeration circuit, including the compressor, plate heat exchanger, expansion valve, and receiver, are modelled based on available templates and parameterized according to manufacturer specifications. This approach primarily employs a 1D formulation, discretized in the flow direction as necessary. For the condenser a model developed by Dusek et al. [15], which takes into account the simultaneous condensation of the refrigerant and the evaporation of the water, is used.

3.4. Vortex Control

To assess the feasibility of vortex control, the ejector is simulated in 3D. However, as shown in Figure 4, injecting nearly 80% of the total mass flow through two tangential inlets reduced the primary mass flow rate by only 2.5%. This modest effect is attributed to the high degree of liquid subcooling, in contrast to the conditions reported by Zhu and Elbel [8]. In single-phase liquid operation, vortex control depends on forming a vapor core that lowers the critical mass flow at the throat. However, strong subcooling suppresses vapor-core formation and therefore raises the required swirl intensity (rotational speed) for onset, as noted by Bodys [9]. Because elevated subcooling is necessary for compressor reliability and to maintain a high COP, reducing it is not a viable option in this system. Consequently, under the present operating conditions, vortex control is ineffective.

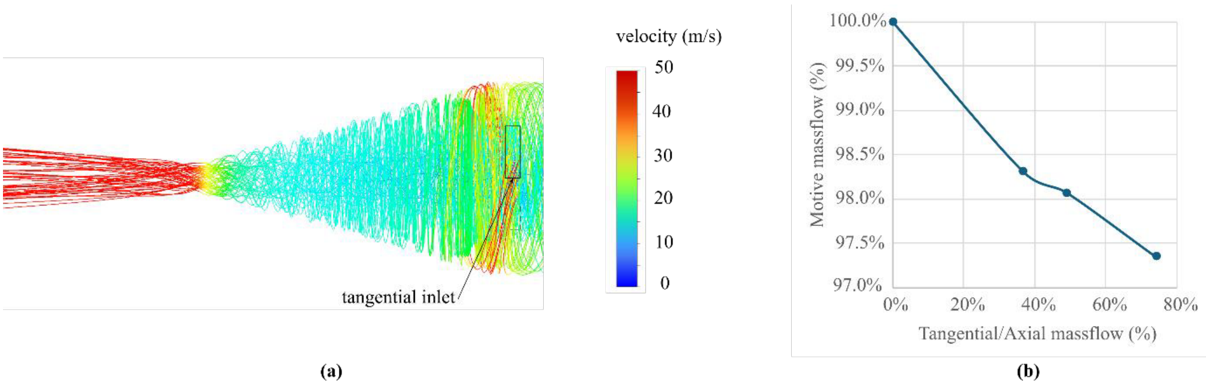

Figure 4. (a) Swirl mass flow control streamlines; (b) dependency of the mass flow on the tangential injected mass flow

3.5. Needle Control

To control the mass flow, a needle with a diameter of 10 mm is designed and inserted into the ejector. Figure 5 (a) illustrates the relationship between heat load Q and the needle insertion distance z, which begins at the throat. In Figure 5 (b), the resulting ejector efficiencies are shown. Since the diverging section of the nozzle is not optimized for lower mass flow rates, the ejector's performance deteriorates under partial load conditions. This degradation becomes particularly problematic around 50% heating capacity, leading to stability issues. To mitigate this, the authors propose incorporating a motive flow bypass at 60% of the ejector's total length. This modification helps to improve operation at 45% load condition. Figure 5 (c) compares the cycle using an ejector with a conventional heat pump cycle. The COP of the standard cycle increases under part load conditions as the temperature differences (ΔT) of the refrigerant in condenser and evaporator decreases, thereby decreasing overall temperature lift in the heat-pump. This effect is contradicted in the ejector cycle by the decrease of the ejector efficiency.

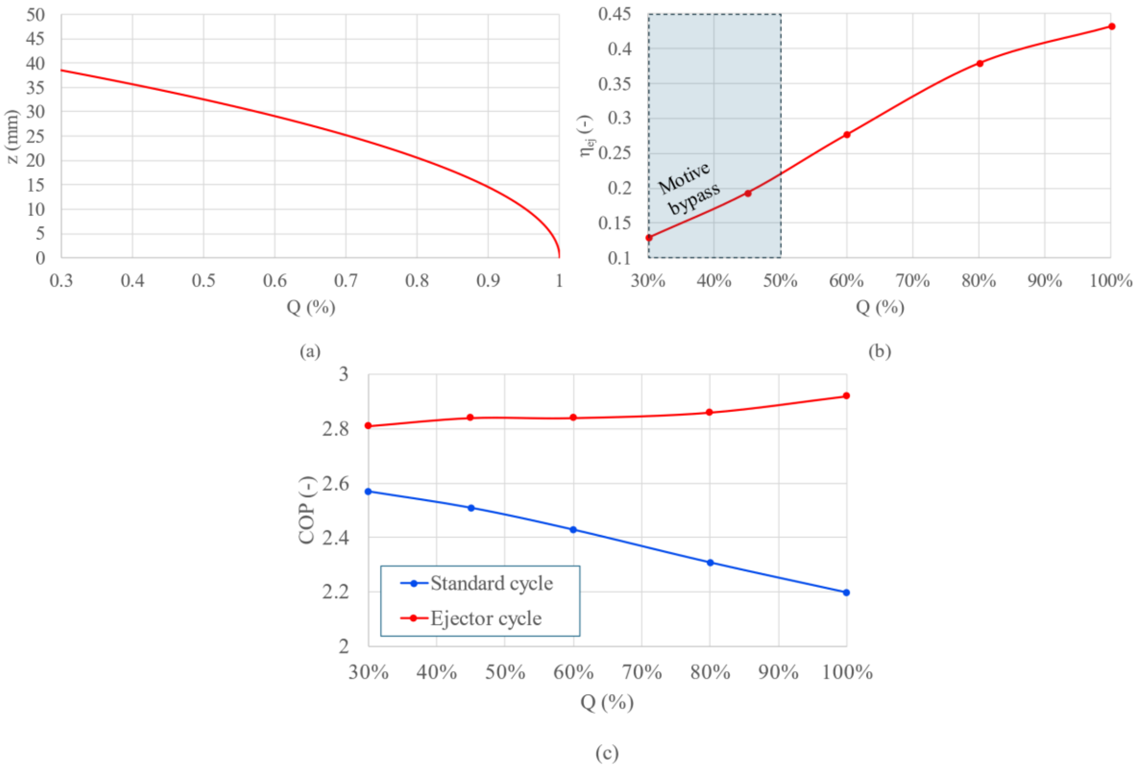

Figure 5. (a) Insertion distance; (b) ejector efficiency; (c) comparison of COP

Figure 6 illustrates the flow behaviour inside the ejector at three different heating capacities. At the design point, the grey coloured needle remains in idle position, and the shock occurs at the outlet of the divergent section of the nozzle. When the load is reduced to 60%, the shock moves further upstream into the nozzle. Although this shift does not significantly affect the ejector performance, it highlights that while the needle position successfully controls the mass flow, the divergent section is not optimized for off-design operation. At heating capacities well below 50%, the situation becomes more critical. For instance, at 300 kW, the shock occurs after only approximately 50% of the divergent section, resulting in ineffective suction and a failure to maintain the desired outlet pressure. Under such low part-load conditions, the authors recommend implementing a primary nozzle bypass to stabilize operation and ensure sufficient suction mass flow.

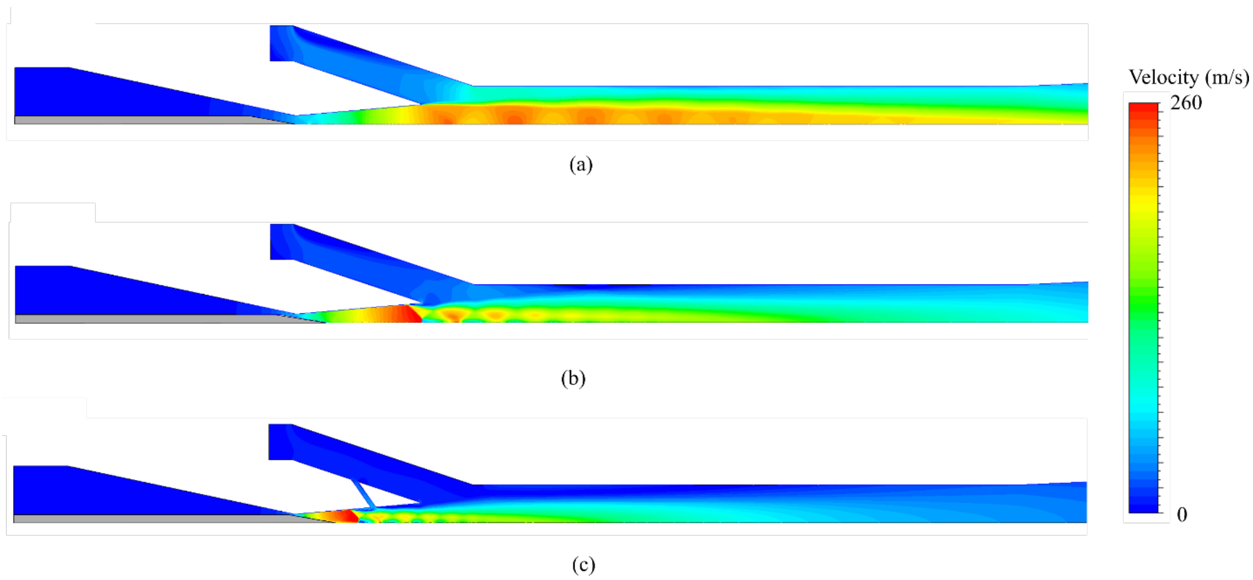

Figure 6. Velocity at (a) Q=100%; (b) Q=60%; (c) Q=30%

However, simulations revealed convergence issues under these conditions, with oscillations of approximately 20% in the suction mass flow. This indicates potential stability and control challenges that require further investigation or system-level mitigation strategies.

3.6. Use-Case Feed-mill

Figure 7 illustrates a typical feed mill process where the heat in now generated by a SGH instead of a gas boiler. Approximately 1 MW of saturated steam at 120 °C is required for conditioning the raw material before it enters the milling stage. After milling, the product is cooled and dried using ambient air, resulting in an excess heat stream of approximately 1000 m³/h at 68 °C and 60% relative humidity (RH). This stream supplies around 650 kW to an intermediate water cycle, which can serve as a heat source for a heat pump. The process is a highly automated batch operation, with cycle durations ranging from 1 to 4 hours, depending on the recipe. The plant operates five days a week, typically experiencing one to three recipe changes per day. Each recipe change takes about 10 minutes, 5 minutes to empty the cooler and 5 minutes to refill it with newly processed material. During the first 5 minutes of a recipe change, waste heat remains available, but no steam is needed, as no product enters the conditioning zone. In the second half of the changeover, the cooler is empty, resulting in no waste heat availability, but the steam is already required. Since heat pumps are not suited for frequent start/stop operation, a smart thermal storage concept is required to make them competitive with conventional gas boilers. To address this, it is proposed to operate the heat pump at partial load during the 10 minutes needed for the changeover. During the first 5 minutes, when the steam is not needed and the steam valve is closed, the shell of the condenser, in which water is evaporated, is used as a short-term steam buffer tank.

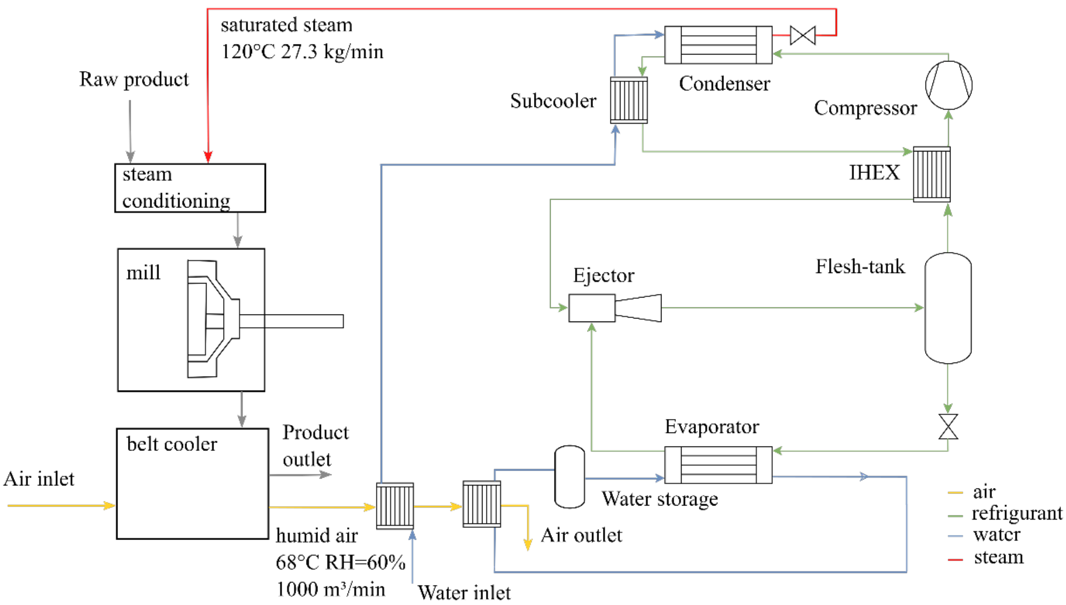

Figure 7. Heat-pump integration in a feed-mill process

There are two ways to use the shell as a buffer storage tank. Steam can be generated and stored directly in the shell of the heat exchanger, which increases pressure in the shell as well as the evaporation temperature of the water and results in increase of the thickness of the shell walls as well as increase of the condensation temperature/pressure of the refrigerant. Alternatively, the mass flow of the inlet water can be increased, so that the evaporation is interrupted, and the heat is stored in additional water as sensible heat. This means a significant reduction in the heat transfer coefficient on the water side, as no evaporation takes place but also an increase in the driving force, as the water in the shell becomes slightly colder. In both alternatives it is necessary to increase the volume of the shell so that it can accommodate either the generated steam (without a significant increase in pressure) or liquid water amount (without overfilling the shell). To sum it up, steam/latent heat storage requires a thicker shell and increased refrigerant condensation pressure, while hot water/sensible heat storage is associated with reduced heat transfer coefficient but slightly increased driving force.

For the studied case, the heat transfer coefficient drop for hot water/sensible heat storage is not as critical as the heat pump only operates under partial load and compared to normal operation, only approximately half of the heat needs to be transferred through the heat exchanger. Moreover, the effect of the drop is counterbalanced by an increased driving force of the heat transfer. The steam/latent heat storage comes with increased refrigerant condensation pressure, and thicker shell walls, which is disadvantageous. Nonetheless, storing the hot water/sensible heat in the shell only saves the energy required to preheat the water in the subcooler. As this energy comes from the refrigerant which needs to be cooled down to achieve sufficient subcooling before entering the ejector anyway, this storage would not benefit the overall process. Therefore, this study considers using the shell of the heat exchanger with increased volume (40% diameter increase) as a short-term buffer tank for steam.

During the second half of the changeover, when there is no heat source available and the steam is needed, a hot water storage tank for intermediate water circuit between humid air and evaporator has to be installed and used to collect hot water for the first half and supply evaporator with hot water for the second half of the changeover. Once the recipe change is complete, the heat pump resumes normal operation.

Figure 8 (a) shows the COP during the product change for three different cases. In the first configuration, indicated by the solid line, the discussed storage concept is applied.

In the second configuration, shown by the dotted lines, the heat pump reduces its power to 30 % during the first five minutes of the changeover, while the generated steam is vented to the environment. In the third configuration, represented by the dashed line, the heat pump operates continuously at the design point, and during the first five minutes of the changeover, 100 % of the generated steam is vented to the environment.

For the COP calculation, the mill's heating demand is used as the useful heat output. At the beginning of the changeover, this demand drops to zero for all configurations during the first minutes, resulting in a correspondingly reduced COP. After this initial period, the storage concept releases previously stored steam, which increases the delivered useful heat and, consequently, raises the COP compared to the other operating strategies.

Figure 8 (b) shows the electrical power consumption of the compressors P and the corresponding heat output Q of the heat pump. Again, the different configurations of the SGH with ejector are compared.

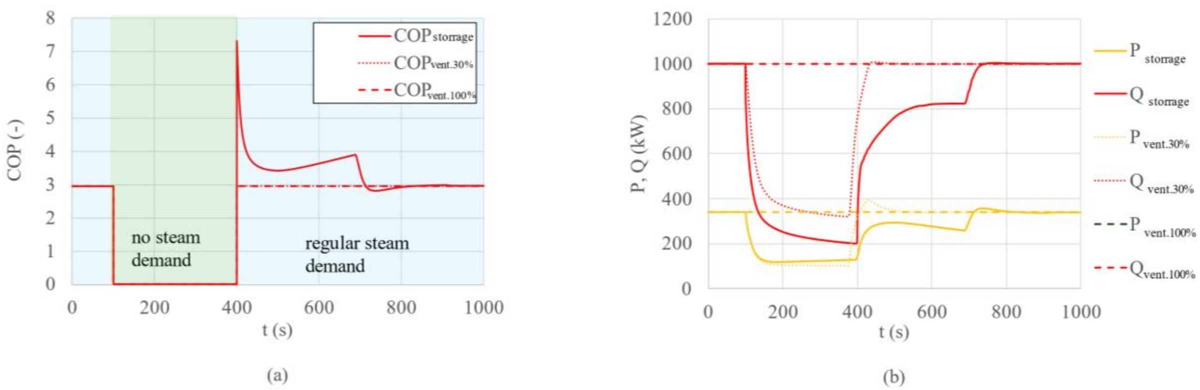

Figure 8. (a) COP during product change; (b) heat load on the condenser and compressor power

For the steam storage case, there is a rapid decrease in heat load at the beginning of no steam demand period. This happens because the compressor is set to the minimum speed, and the heat transfer coefficient decreases as the evaporation is not that rapid and the water is not mixed as much. The power of the compressor goes down when the speed is set to minimum and then goes up slowly as the refrigerant condensation temperature/pressure goes up to suffice for water evaporation temperature/pressure going up. After five minutes, the compressor switches to medium speed. This is because there is less power needed at this point, as there is steam stored in the evaporator shell and is being used. Pressure in the shell as well as pressure of the refrigerant goes down during this time, which causes slight decrease in the compressor power. Heat load increases accordingly and stays well below 1 MW as the stored steam is being used. Shortly before the changeover ends, the compressor speed is regulated to reach the required heat load after the changeover.

In comparison, in the case without steam storage, heat load does not drop so much at the beginning of the changeover as the evaporation/condensation pressure of the water/refrigerant does not increase for this case. However, all the steam is vented, and energy is lost. Regarding the compressor power, it goes down as the speed is set to minimum and stays constant for the no steam demand period, as the condensation pressure of the refrigerant/the compressor outlet pressure stays the same. Shortly before the period of no steam demand ends, the compressor is regulated to reach 1 MW heat load.

The storage concept reduces energy consumption by roughly 20% compared to the venting strategy operated at 30% heat load, and by approximately 70% compared to venting at 100% heat load.
Figure 8 (d) shows a simple Net-present Value (NPV) calculation considering a natural gas to electricity price ratio of 2.6 with additional CO_2 costs of 80€/t. The interest rate was set to 5% per year and the heat-pump costs to 600€/kW with an ejector cost assumption of around 65€/kW based on prototype offers. The introduction of the storage concept makes the solution technically feasible; however, improving the COP by adding an ejector is essential to fulfil economic targets (ROI < 5) and push the technology toward practical application.

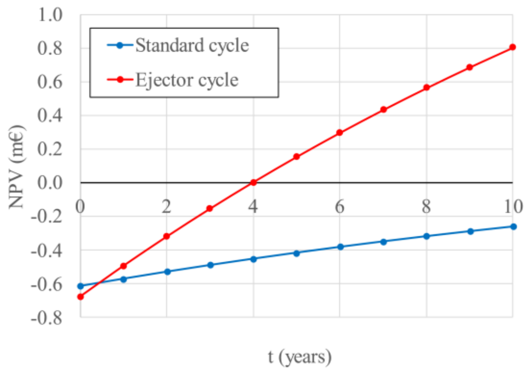

Figure 9. NVP of the Standard cycle compared to the ejector cycle

4. Conclusion

An ejector for a steam-generating heat pump is designed using CFD simulations based on a homogeneous equilibrium model. To accommodate part-load operation, various strategies were evaluated. The results indicate that integrating a needle into the motive nozzle is the most effective approach for reducing the heat capacity while maintaining performance. However, high subcooling—often used to optimize the overall COP—was found to impair the effectiveness of swirl control within the ejector.
The simulations of the needle ejector demonstrated stable operation down to approximately 50% of full heat capacity. Below this threshold, geometric mismatches in the divergent section of the ejector become too significant to be managed effectively. To achieve further reduction in heat capacity without resorting to multi-ejector systems, the implementation of a motive nozzle bypass is proposed as a viable solution.
The potential of the solution is demonstrated on a real-world feed mill use case. Since this is a batch process, a storage concept is introduced to ensure the technical feasibility of implementing a heat pump for handling recipe changes. The results from the use-case indicate that improving the Coefficient of Performance (COP) by incorporating an ejector is critical to meeting the economic targets (ROI < 5 years) and advancing the technology toward practical application.
The next step is to demonstrate the practical application at the prototype level in a laboratory setting, before moving on to real-world applications. Future work will focus on developing more advanced numerical approaches that incorporate non-equilibrium thermodynamics to support the design of a flexible ejector and optimize the overall system.

Acknowledgements

This publication was conducted within the project "VLESH" (FFG project number: 914844).
This project is funded by the Austrian national Research Funding Agency (FFG).

Nomenclature

Abbreviations

CFD	Computational Fluid Dynamics
COP	Coefficient of Performance
HEM	Homogeneous Equilibrium Model
SGHP	Steam generating heat-pump
UDF	User Defined Function
UDS	User Defined Scalar

Greek Symbols

Δ	Deviation
η_{ej}	Ejector efficiency
Γ	Diffusion coefficient
λ	Thermal conductivity
μ	Dynamic viscosity
μ_t	Turbulent viscosity
ϕ	Spare variable
Π_s	Suction pressure ratio
ρ	Density
σ_t	Turbulent Prandtl number

Latin Symbols

c_p	Specific heat capacity at constant pressure
D	Diameter
h	Specific enthalpy
K	Turbulence kinetic energy
L	Length
$\dot{m}$	Mass flow rate
NVP	Net present value
P	Compressor power
p	Pressure
r	Radius
r, θ, z	Direction vector components in cylindrical coordinates
s	Specific entropy
$\dot{S}$	Source term in transport equation
$\boldsymbol{u}$	Velocity vector
x, y, z	Direction vector components in cartesian coordinates
X	Entrainment ratio

Subscripts:

0	Initial state
DIF	Diffusor
ej	Ejector
MIX	Mixing chamber
MN	Motive nozzle
out	Outlet
SN	Suction nozzle

References

[1] Koundinya, S., & Seshadri, S. (2022). Energy, exergy, environmental, and economic (4E) analysis and selection of best refrigerant using TOPSIS method for industrial heat pumps. *Thermal Science and Engineering Progress*, *36*, 101491.

[2] Kornhauser AA. (1990). The use of an ejector as a refrigerant expander. Proceedings of USNC/IIR-Purdue refrigeration conference, USA.

[3] Elbel, S. & Lawrence, N. (2015). Review of recent developments in advanced ejector technology. International Journal Of Refrigeration, 62, 1–18. https://doi.org/10.1016/j.ijrefrig.2015.10.031

[4] Lawrence, N. & Elbel, S. (2015). Mathematical modeling and thermodynamic investigation of the use of two-phase ejectors for work recovery and liquid recirculation in refrigeration cycles. International Journal Of Refrigeration, 58, 41–52. https://doi.org/10.1016/j.ijrefrig.2015.06.004

[5] Lawrence, N., & Elbel, S. (2019). Experimental investigation on control methods and strategies for off-design operation of the transcritical R744 two-phase ejector cycle. *International Journal of Refrigeration*, *106*, 570-582.

[6] Grazzini, G., Milazzo, A., & Mazzelli, F. (2018). Ejector Design. In Ejectors for Efficient Refrigeration: Design, Applications and Computational Fluid Dynamics. Springer.

[7] Elbel, S. and Hrnjak, P. (2008). Experimental validation of a prototype ejector designed to reduce throttling losses encountered in transcritical R744 system operation. International Journal of Refrigeration, 31(3):411–422. http://dx.doi.org/10.1016/j.ijrefrig.2007.07.013

[8] Zhu, J., & Elbel, S. (2020). Experimental investigation into the influence of vortex control on transcritical R744 ejector and cycle performance. *Applied Thermal Engineering*, *164*, 114418.

[9] Bodys, J., Smolka, J., Palacz, M., Haida, M., Banasiak, K., Nowak, A. J., & Hafner, A. (2016). Performance of fixed geometry ejectors with a swirl motion installed in a multi-ejector module of a CO2 refrigeration system. *Energy*, *117*, 620-631.

[10] Unterluggauer, J., Buruzs, A., Schieder, M., Sulzgruber, V., Lauermann, M., & Reichl, C. (2025). Design of Ejectors for High-Temperature Heat Pumps Using Numerical Simulations. Processes, 13(1), 285.

[11] Schieder, M. (2023). Characterization and Optimization of Ejectors using Numerical Fluid Dynamics. Master's Thesis, TU Wien, Wien, Austria

[12] Smolka, J., Bulinski, Z., Fic, Z., Nowak, A. J., Banasiak, K., and Hafner, A. (2013). A computational model of a transcritical R744 ejector based on a homogeneous real fluid approach. Applied Mathematical Modelling, 37(3):1208–1224. http://dx.doi.org/10.1016/j.apm.2012.03.044.

[13] Lemmon, E. W., Bell, I. H., Huber, M. L., and McLinden, M. O. (2018). NIST Standard Reference Database 23: Reference Fluid Thermodynamic and Transport Properties-REFPROP, Version 10.0, National Institute of Standards and Technology

[14] ANSYS, Inc. (2022). Ansys® Fluent Theory Guide, Release 2022 R1. Canonsburg, USA, 2022.

[15] Dusek, S., Lauermann, M., Helminger, F., & Wilk, V. (2021). Analysis of a steam generating high temperature heat pump for industrial waste heat recovery. In 13th IEA Heat Pump Conference.